Progress of Theoretical Physics Vol. 84, No. 2, August 1990

Metastable States of the Fuzzy Spin Model. I

—— *Static Structure* ——

Tatuo KAWASAKI

Physics Department, College of Liberal Arts and Sciences, Kyoto University, Kyoto 606

(Received Aplil 5, 1990)

A new spin system, in which spins are random in their magnitudes, is proposed to get a further insight into structure and property of the metastable states in random spin systems. Numerical analysis is used to examine the metastable states, which are found almost heavily degenerated and have fairly stable many-valley structures though the system is inherently unfrustrated. Metastable configuration of the spins is considerably ramified and stability of the metastable states is mainly attributed to network structure composed of bigger spins in their magnitudes.

§ 1. Introduction

The aim of this paper is twofold: Introducing a new random, unfrustrated spin model[1)~3)] we first engage in clarifying further the role of the metastable states in the frustrated systems, like spin glasses. In particular we will concern ourselves with toughness of the states against perturbations. At the same time we hope to show that the new spin model is appropriate not only for studying the metastable states, but also for revealing a new feature of the random system.[1)~3)]

The many-valley structure of the energy surface gives us the impression that it is unique in the spin glass, the frustrated system. The sructure is formed on the existence of a large number of almost degenerated, metastable states in the free energy. However the frustration is proved enough but unnecessary for generating degenerated states in several articles;[1),4)~6)] a random but unfrustrated system can also have an energy surface with many-valley structures. We therefore wish to concentrate here on clarifying the relation between randomness and abundance of metastable states in the system. Our previous papers[1)~3)] give preliminary reports on the structure of the metastable states using the new random spin model, *the fuzzy spin model.* In this report discussion on the states will go further, associated with dynamical aspects of them.

In § 2 the random model introduced in this report is discussed in comparison with other random models. In §§ 3 and 4 numerical analysis is performed with the aid of Monte Carlo Method. Properties at 0 K is discussed in § 3 and toughness of the states is examined in § 4. In the last section, § 5, a summary is given and a preliminary report on phenomena at finite temperatures is presented, The ordering temperature is also determined.

§ 2. Model

The new random spin model is defined by the Hamiltonian[1)] ($\sigma_j = \pm 1$),

$$H=-\sum_{<ij>} J_{ij}s_is_j\sigma_i\sigma_j\,, \tag{1}$$

where the s_j's stand for the Ising spin operators whose magnitudes in principle vary site by site and are governed by a characteristic distribution function discussed below. Introducing a new scalar random variable ξ by the relation that

$$s_j=S\xi_j\,, \tag{2}$$

under the assumption that the spin has a maximum magnitude S, we will rewrite the Hamiltonian in the following form:

$$H=-S^2\sum_{<ij>} J_{ij}\sigma_i\sigma_j\xi_i\xi_j\,. \tag{3}$$

Relations between models

The range of the variable ξ is then limited between 0 and 1. Property of ξ determines character of the model since the variable ξ governs the variety of spin magnitude changing site by site in the Hamiltonian. For example, in a diluted magnet the variable ξ plays a role of an indicator of site occupancy: ξ should be assigned to 1 (or 0) for each occupied (or vacant) site. When the variable ξ takes ±1, the model becomes the Mattis one.[8]

In the concept of bond-randomness, the pair product $\xi_i\xi_j$ should be replaced by a new random variable η_{ij} defined by

$$J_{ij}\xi_i\xi_j\longrightarrow J_{ij}\eta_{ij}\,. \tag{4}$$

When the variable η_{ij} takes ±1 randomly at a given rate, it gives the $\pm J$ model, widely used in studying spin glasses. When the η_{ij}'s are positive (or negative) definite and random, the model is then called a random ferro (or antiferro) magnet (FRM).[4)~6)] When η_{ij} takes only 0 and 1 at some probabilities, the model corresponds to the bond-diluted random magnet.

Here we will characterize the model by introducing a distribution function of the random variable ξ, which defines frequency of ξ_j. Spin magnitude at each site is then assigned randomly following the function. The value is not necessarily restricted to discrete ones, but can be continuous as is seen in Fig. 1. This is a straightforward

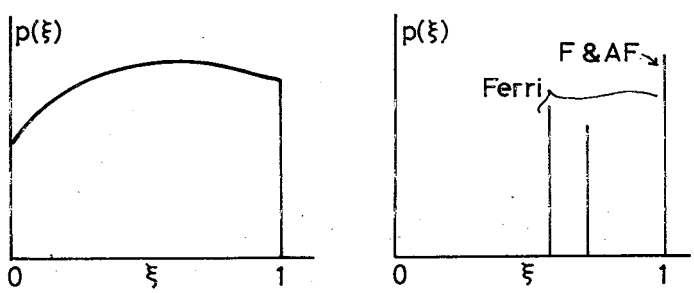

Fig. 1. Characteristic distribution function of ξ. The value ξ_j at the site j is determined with probability defined by this function. For ferro- and antiferro-magnets, the function is the delta-function at $\xi=1$ while for ferrimagnets it is composed of several delta-functions corresponding to magnitude of spins.

extension of the random magnets where ξ takes only 0 or 1 randomly. In the standard magnets, that is, in ferro- and antiferro-magnets, the function is something like the delta-function, as is seen in Fig. 1.

Model used here

In the present model discussed here, we will adopt a uniform function between 0 and 1. We call the present model the *Fuzzy Spin Model* (FSM)[1] in the sense that the spin magnitudes can have any values randomly and continuously between 0 and S site by site. For simplicity the coupling J_{ij} is hereafter assumed effective only between nearest neighbor pairs ($J_{ij}=J>0$).

By definition the system is essentially ferromagnetic and should therefore have a unique ground state at zero temperature. The transition temperature T_c is given by, in the molecular field theory,

$$k_B T_c/J = zS^2/4 \tag{5}$$

since the average value of ξ_j should be 1/2 from the definition. All sites have magnetic spins, however small spin magnitude at each site may be. Therefore all sites are necessarily connected/correlated in the present model, resulting in no percolation problem in spite of the random nature of the model. It is however noted that spin-spin correlation is definitely weaker than that of the standard Ising model due to the existence of vanishingly small spins.

Suppose now that in a chain model there are two spin clusters, adjacent to each other, centered with antiparallel big spins respectively and forming mutually antiparallel domains. (See Fig. 2.) Probability is in general small at low temperatures for the bigger spins to overturn parallel with each other and to coalesce into a single domain.

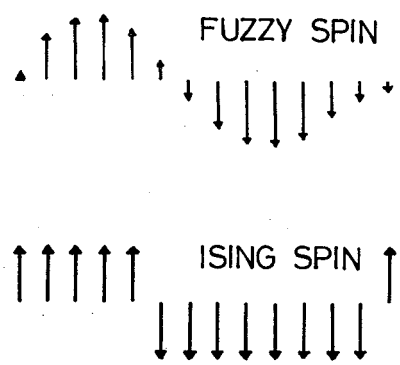

Fig. 2. Antiparallel domains in one-dimensional spin system. A typical stable domain structure is shown where bigger spins are surrounded by smaller spins. The bigger spins are stable against perturbations from other-domains while no extra energy is required for the Ising spin domains to propagate flipping at the domain boundaries.

The situation is completely different from that of the usual Ising model in that the fuzzy model needs extra energy in forming a single domain from a multiple domain stucture even in the one dimensional system. As will be realized in the following simulation, this situation will be found true even in the two-dimensional system and be concluded as one of the main physical reasons for the model to have lots of metastable states at low temperatures.

In the one-dimensional case exact analytical expression for the partition function can be obtained as is shown in the Appendix where internal energy and specific heat are also derived.*) It shows that the equilibrium properties are not different qualitatively from those

*) Professor O.Nagai kindly suggested the author possibility of deriving analytic expression of the partition function and sent him the same results shown in the Appendix.

of the Ising system.

§ 3. Realisation of metastable states at 0K

The subsequent simulation is carried out on the two-dimensional square lattice with the aid of the usual Glauber's one-spin-flip dynamics. The Exclusive-OR operation is used to produce the random numbers needed in the simulation. The model is set by assigning the random number [0,1] to ξ_j as the initial spin configuration. The machine FACOM VP-400E was mainly used for computations, with several test runs for the same programs by the machine FACOM-782.

Pattern due to metastable states

Metastable states are found in various systems when the variation rate is too fast for the system to follow the change of its surroundings. From the microscopic point of view, smaller spins are apt to turn to the same direction of their nearest bigger spins at the initial stage of quenching to lower temperatures and to form domains centered at the bigger spins. In Fig. 3 one of the spin patterns (90×90) is shown with its structural pattern composed only of bigger spins ($s\geq0.75S$). These are obtained, using the Monte Carlo Method, by quenching from the infinite temperature to 0K. (Hereafter an abbreviation '0-TQ' is used for this process.) A few hundred steps are found enough to get final configurations, in which any one-spin-flip from them needs extra energy. Black and white dots stand for up- and down-spins, respectively. Size of each spot, though hard to discriminate it, corresponds to magnitude of the spin at the site. The true equilibrium state should be, as is mentioned above, ferromagnetic; the spin pattern consists of a single domain. The configuration shown here therefore should correspond to that at one of the metastable states the system can have. The network of bigger spins is clearly seen in the bottom figure. In the 0-TQ, subsequent new spin configurations are selected by the rule that the lower energy state is always preferred for a considered spin at each step and no fluctuations are taken into account. It

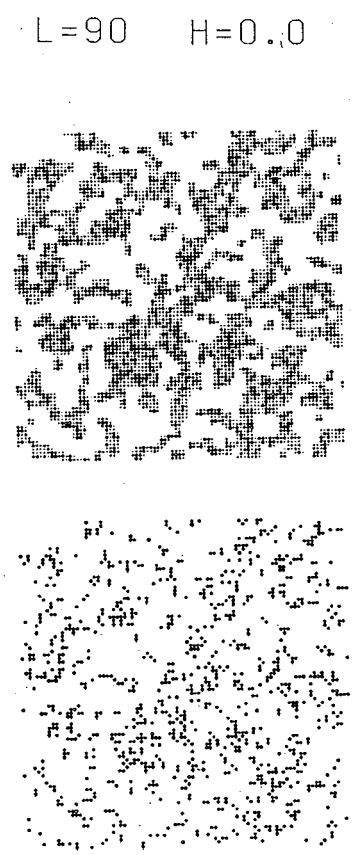

Fig. 3. A final spin pattern (90×90) under quenching from the infinite temperature to 0K. True equilibrium configuration is ferromagnetic while the pattern shows vanishing total magnetization. The bottom figure shows structure of the pattern composed only of bigger spins ($s\geq0.75$).

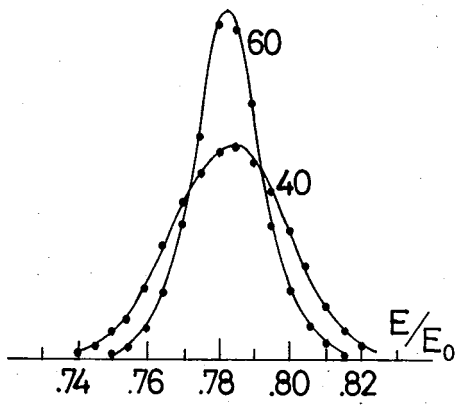

Fig. 4. Frequency distribution of the metastable energy states in 40×40 and 60×60 lattices. The central peaks locate at about 0.79×(the ground state energy E_0). The curves are almost Gaussian.

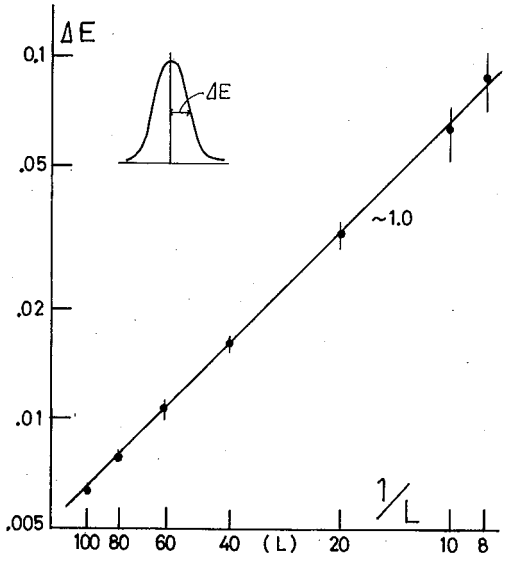

Fig. 5. Width of the Gaussian curves versus sample size L. Linear dependence suggests that the width goes to zero with increasing sample size L. It means complete degeneracy is achieved in the infinite lattice.

therefore means that the quenching routes induced by different random number sequences will generate, at high probabilities, different metastable states. This should be one of the main reasons why the present model is rich in highly degenerated metastable states when the system is quenched to low temperatures.

Energy distribution

Using 10 different initial spin configurations in the lattices of 40×40 and 60×60, frequency distributions of the metastable energy states are plotted in Fig. 4, where 10000 trials are carried out for each different sample. In these trials the same states are scarcely found due to the *fuzzy* character of the model where none of spins have the same magnitude. The peaks locate near at 0.79× (the true ground state energy E_0), which is comparable with the value 0.747 of FRM.[4] Other lattices give 0.80 for 10×10, 0.77 for 20×20, and 0.79 for 80×80 and 100×100 in the present simulation. The result has a similar nature to that of the frustrated spin glasses in that both distribution curves are sharp around their centered values, meaning a large number of states lie in a narrow energy region as in the case of spin glasses.[9),10)] The curves are nearly gaussian with the same peak position $0.79\times E_0$ within statistical errors. Reduction of the energy from E_0 is due to small cancellation coming from the boundary (surface) of domains where antiparallel spin-pairs are formed mainly with smaller spins. As will be shown later in Fig. 7, fraction of the boundary spins is about 0.3. Width of the curves is plotted versus sample size L in Fig. 5. Linear dependence to system size $N(=L\times L)$ shows us that the metastable states will become completely degenerated in the limit of the infinite size. In other words, energy differences between any two nearest metastable states E_1 and E_2 will reduce vanishingly small as the system size goes to infinity.

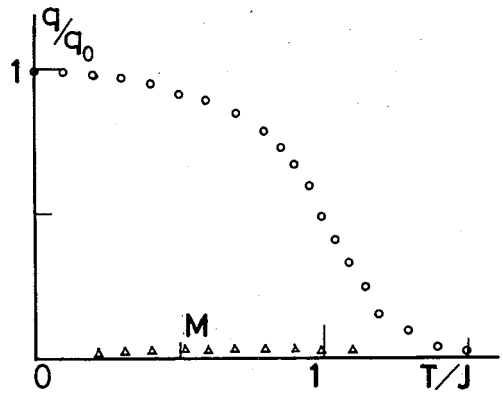

Fig. 6. Temperature dependence of magnetization and spin-glass order parameter defined by $\langle\langle S\rangle^2_{\text{time}}\rangle_{\text{system}}$ when the sample is quenched to each temperature from the infinite one. Only 2×10^4 MCS (60×60) are used during which the quantity q becomes already steady. Equilibrium state is not yet attained while freezing of spins is already established (cf. Fig. 4 of Ref. 2)).

$$\lim_{L\to\infty}(E_2-E_1)=0 \text{ as } 1/L\,. \tag{6}$$

Or, it means that the bottom of many-valleys will have the same energy in the system free energy surface though the barrier heights are not known. Through the quenching processes total magnetization of the system is found nearly zero even at the final temperature 0K while the so-called spin-glass order parameter defined by $q(\equiv\langle\langle S^z\rangle^2_{\text{time}}\rangle_{\text{system}}$ grows up to 1/3 (the maximum value in the present model) as is seen in Fig. 6.[1)~3)] The latter is due to a completely frozen configuration of spins trapped at one of the metastable states without fluctuations in energy and magnetization at 0K. Hence the present metastable states will correspond to one of the minima of the constraint total free energy in magnetization. Behavior of the parameter q suggests existence and order of a phase transition temperature of the system when it is gradually cooled. As far as the 0-field quenching process is used, the results are unchanged in the simulation less than 10^5 MCS in the lattice 60×60. The system may be rich in metastable states. Longer trials will be discussed at the subsection *Relaxation* in the next section.

Shape of clusters

One more difference from the Ising model is on shapes of clusters. Namely, the clusters are, as is seen in Fig. 3, not compact in their shapes, rather ramified like clusters at the percolation threshold. To measure complexity of the shapes, we counted total number of broken bonds defined as bonds with antiparallel spins at both ends. This will give a rough estimation to the total surface length of the clusters; for more detailed statistics we should consider surfaces cluster by cluster. The number of the broken bonds N_b is then found proportional to the total sites $N(=L\times L)$ fairly well as is seen in Fig. 7. Namely, the surface length of the clusters is proportional not to linear dimension of the system but to the size N itself. It means that the clusters are, not compact, rather ramified in their shapes. The linear dependence also suggests that degree of ramification of clusters is kept constant as the system size goes to infinity. This assures the constant peak location in the energy distribution of Fig. 4 above. Nearly degenerated metastable states is strongly related with this ramification since a simple pattern with compact clusters will yield only a few discrete energy states. Fraction of the broken bonds is found 0.31 to the total bonds, which should be compared with 0.345 in FRM.[4)] A completely frustrated system will have broken bonds comparable to the system size.

Internal fields

Distribution of internal fields at the metastable states (60×60) is plotted in Fig. 8 where the positive field side only is drawn owing to symmetry. The distribution is sharply limited between $-zJS$ and $+zJS$ since the maximum value of the field strength is zJS ($=4JS$ here). The curve has a peak at around $2JS$, which is estimated nicely by the mean field theory as $zJ<S>(=2JS)$. Finite height at 0 field is characteristic of the degenerated metastable states since the stable ferromagnetic state is expected at 0K by the definition of the model. Namely, the slow-cooling of the system does give the curves inserted, in which numerals attached indicate temperatures scaled by T_c. To get the latter curves, average is taken over 7×10^4 MCS after equilibrium is achieved in the sample 36×36. Below T_c the curves have no symmetry with $h=0$: The curve at $T=0.19$ has no counterpart in the negative field side. By the way, magnitude of the 0-field in the original figure corresponds to fraction of free spins which can flip at no cost of energy. It should, however, be noted that there are no spins with zero internal field in a strict sense since none of them are similar and no exact cancellation is expected in the fuzzy spin model. Though with this restriction,

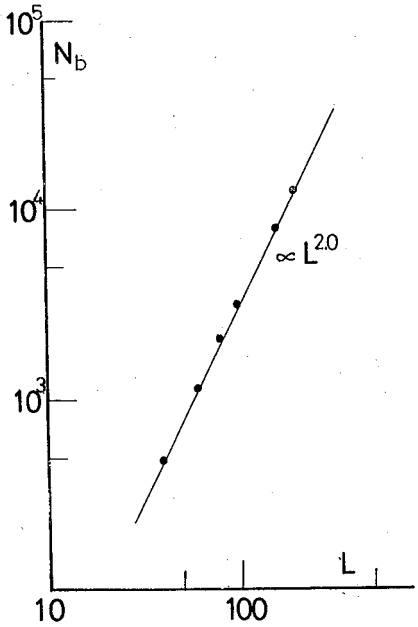

Fig. 7. Number of broken bonds versus sample size. Square dependence that the number N_b is proportional to area of the clusters means they are well ramified as those at the percolation threshold. Their fraction is 0.31 ($N_b=0.31N$).

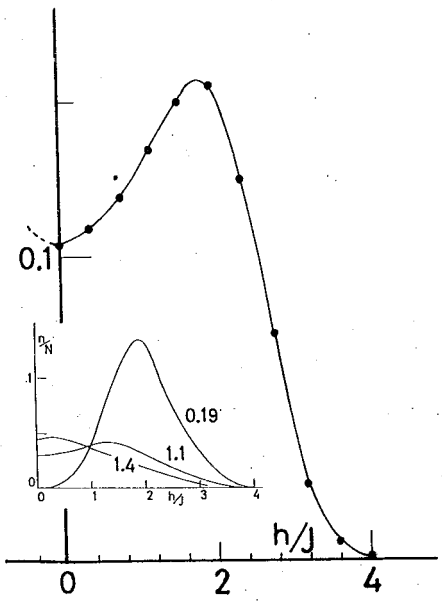

Fig. 8. Distribution of internal fields. Distribution curve is drawn on the basis of histogram (10 divisions in [0,4] J). The spin S is set unity. Non-zero height around 0 field means degeneracy of energy states due to nearly free spins at the metastable states (cf. Fig. 4 of Ref. 1)). The figure inserted indicates the field distribution at finite temperatures scaled by T_c. It clearly shows no height at 0 field at low temperatures in the equilibrium state: The non-zero height is characteristic of the existence of the metastable states.

the distribution suggests that the metastable states of the model are considered to be heavily degenerated in a wider sense since the portion of the nearly-zero field is meaningly large. If we divide the range of fields into 10 equal sections, ratio of the area around the zero field to the total is about 12%, which may be related with density of the metastable states.[1)]

§ 4. Toughness of metastable states

Status of individual spins at 0K

We have shown in the previous section that the spin configuration at the metastable state has a stable structure formed with bigger spins and has no total magnetization when the system is quenched to lower temperatures. Stability of the states therefore will depend critically on behavior of the bigger spins. We divided spin magnitude into three classes and traced them individually after quenching. In Table I, we listed fractions of unflipped spins keeping their initial directions after the quenching process ended. The data are obtained after averaging over 10000 trials starting at one initial configuration (60×60). Typical ranges of spins are selected for this purpose: Big ($0.95\sim1.0$) stands for spins in the range between $0.95S$ and $1.0S$ and so forth. It seems reasonable in the standard Ising model that possibility of keeping their original directions is fifty-fifty after having quenched. Hardness of flipping in the bigger spins plays an important role in forming the network structure of the final spin pattern. This also helps the system to persist vanishing magnetization even at low temperatures in that the initial random configuration of the bigger spins are almost kept in their up-down directions. Therefore one of the metastable states is once realized at 0K, it is fairly stable in that bigger spins cooperate with each other to keep rigid backbone structures. This property is also of the characteristics in the fuzzy spin model, which is not seen in the usual Ising model.

Table I. Fraction of unflipped spins. Abbreviations Big, Mid and Sml stand for portions of spins belonging to magnitudes indicated in parentheses respectively. The largest magnitude is scaled to 1. The numeral tabulated shows fraction of unflipped spins in each class when the 0-temperature quenching process is performed in the lattice 60×60.

	Fuzzy	Ising
Big(0.95~1.0)	0.70	
Mid(0.475~0.525)	0.49	0.50
Sml(0.0~0.05)	0.53	

Relaxation

Existence of metastable states usually affects relaxation processes in an essential way: The process is often disturbed and prolonged by being trapped or staying at some of the metastable states. In the simulation experiments the metastable states are practically defined as the states which have extraodinarily longer relaxation time. In Fig. 9 the relaxation behaviors of both the present model and the Ising model are compared, where quenching is performed from infinity to $0.90T_c$ in both models. Without magnetic fields the fuzzy model needs more than 10^5 MCS to get to its equilibrium state while only a few hundreds MCS are enough for the Ising model. Even with a magnetic field of $0.1J$ which is strong enough for the Ising model to get a fully magnetized state, the required steps are still comparable with those of no

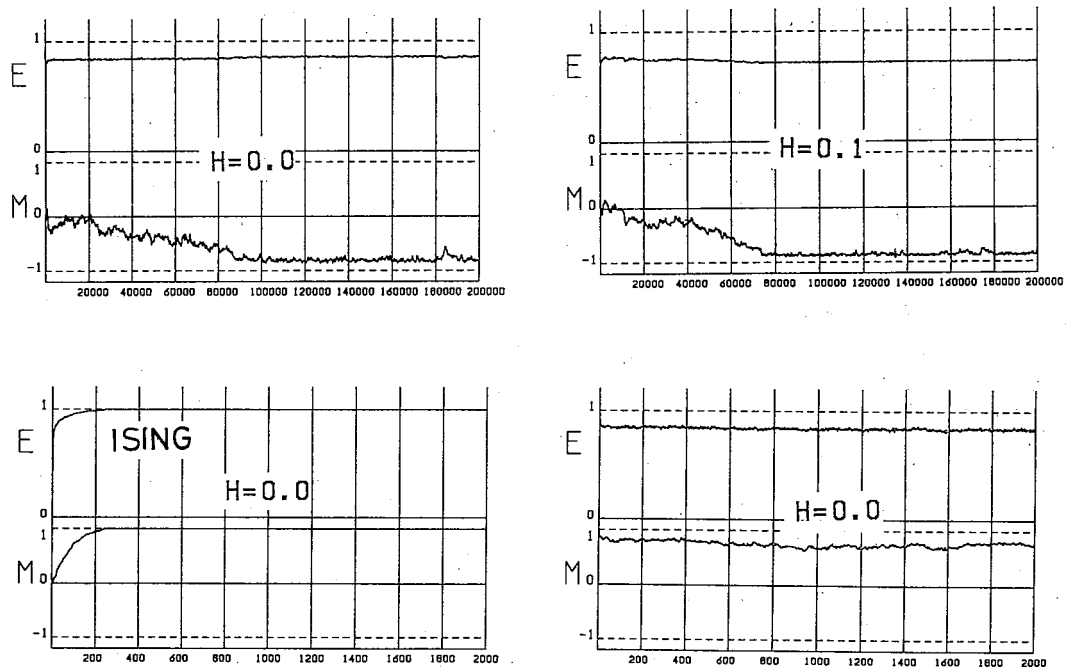

Fig. 9. Behavior of relaxation to true equilibrium states at $0.9T_c$. The system is quenched from infinite to the temperature. The fuzzy model requires more than 10^5 MCS before being in the equilibrium state while several hundreds MCS are enough for the Ising model (the left figures). The situation does not change even under the field-cooling process (the right upper figure). In the right bottom figure the quenching is performed from the true ground state to the temperature, which shows a short ralaxation.

magnetic field in the fuzzy model. This cannot be attributed only to the difference of effective coupling strengths (Ising: Fuzzy=1: 0.25). Some metastable states are not so shallow in the fuzzy model that the field $0.1J$ seems not enough for the system to overcome energy barriers.

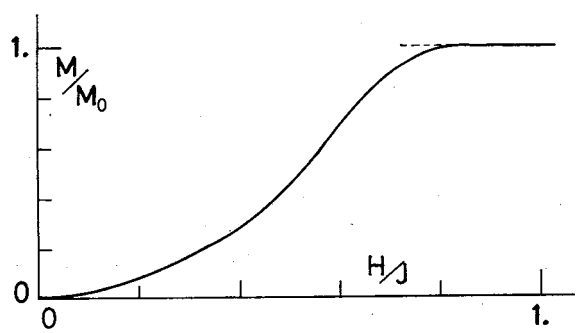

Fig. 10. Magnetization obtained by the field-cooling. The quenching is performed from the infinite to 0K. Fully magnetized state is achieved only under a field comparable to the exchange strength J (cf. Fig. 6 of Ref. 1)).

Field dependence

Total magnetization is studied through the 0-temperature field-cooling process: The magnetization resulted depends strongly on the applied field strength due to the existence of the metastable states. The dependence is shown in Fig. 10 where the field-cooling is carried for a sample (60×60) and 1000 trials are averaged to get the figure. The fully magnetized state is obtained only under a field strength comparable with the coupling constant J. Suppose that there located a pair of big spins which have unfavorable

directions in the applied field. Then energy comparable with J is required when one of pair spins flips with the aid of the field. It means that some of the energy barriers for big spins are as high as the exchange coupling strength J. This also indicates that field-induced reconstruction of the once obtained pattern is hard since flipping of the bigger spins require higher fields.

Thermal stiffness

Annealing the system is one of the powerful procedures to ride over barrier heights for spin flipping. We examined the stability of the patterns by the following steps: First the system is prepared by the 0-TQ. Then it is annealed at a given temperature. The number of unflipped spins after processed is estimated as an indicator of toughness of the spin configuration to thermal disturbances. Four annealed temperatures are selected; $0.1J$, $0.3J$, $0.5J$ and $1.1J$. Spin patterns are shown in Fig. 11, where top maps show ordinary spin configurations and bottom ones their skelton patterns which are plotted using only with bigger up-spins ($0.75S \sim 1.0S$). Toughness of the metastable states is, at a glance, realized in the stable skelton patterns. Even at $T=0.5J$ the skelton pattern after annealing for 2×10^5 MCS still resembles considerably well with that at 100 MCS in Fig. 12. Since spins here are completely dissimilar with each other, the pattern is not flexible for deforming itself and never shift as a whole; this is not true in the Ising model. This situation will therefore restrict ralaxation paths to change the states, resulting in helping persistency of the metastable states. It is surprising that the total magnetization still remains about 10% of the equilibrium value even after 2×10^5 MCS and seems steady in time though the system reaches, without doubt, the true equilibrium ultimately. Further discussion will be presented elsewhere.

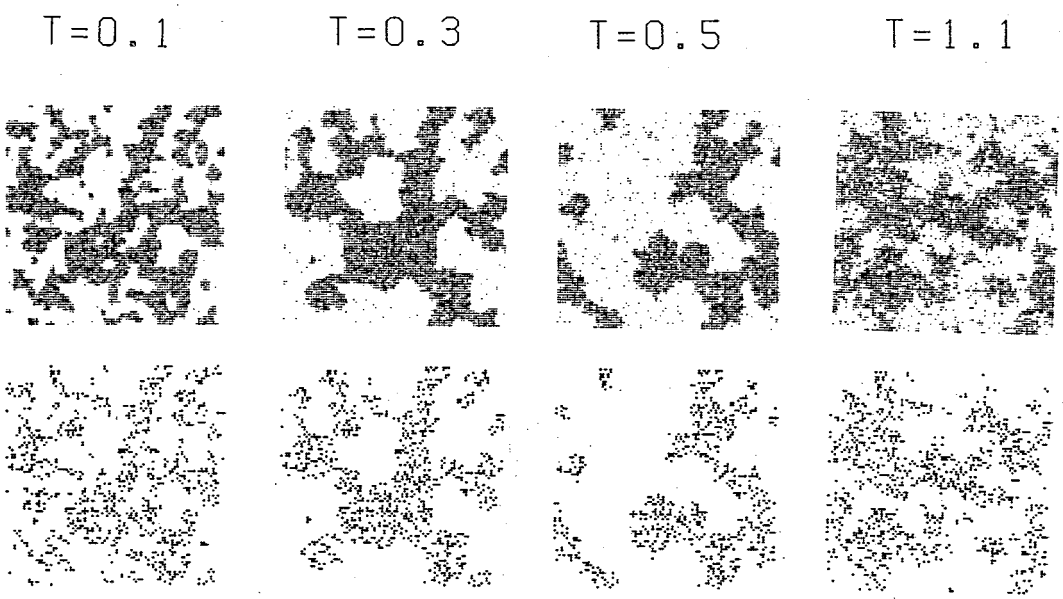

Fig. 11. Annealed pattern after quenched to 0K. Patterns of the backbones (patterns of bigger spins) are shown at the bottom. Annealing at low tempertures is not sufficient to overcome barriers between the metastable states once obtained. The beginning pattern should be referred to Fig. 12.

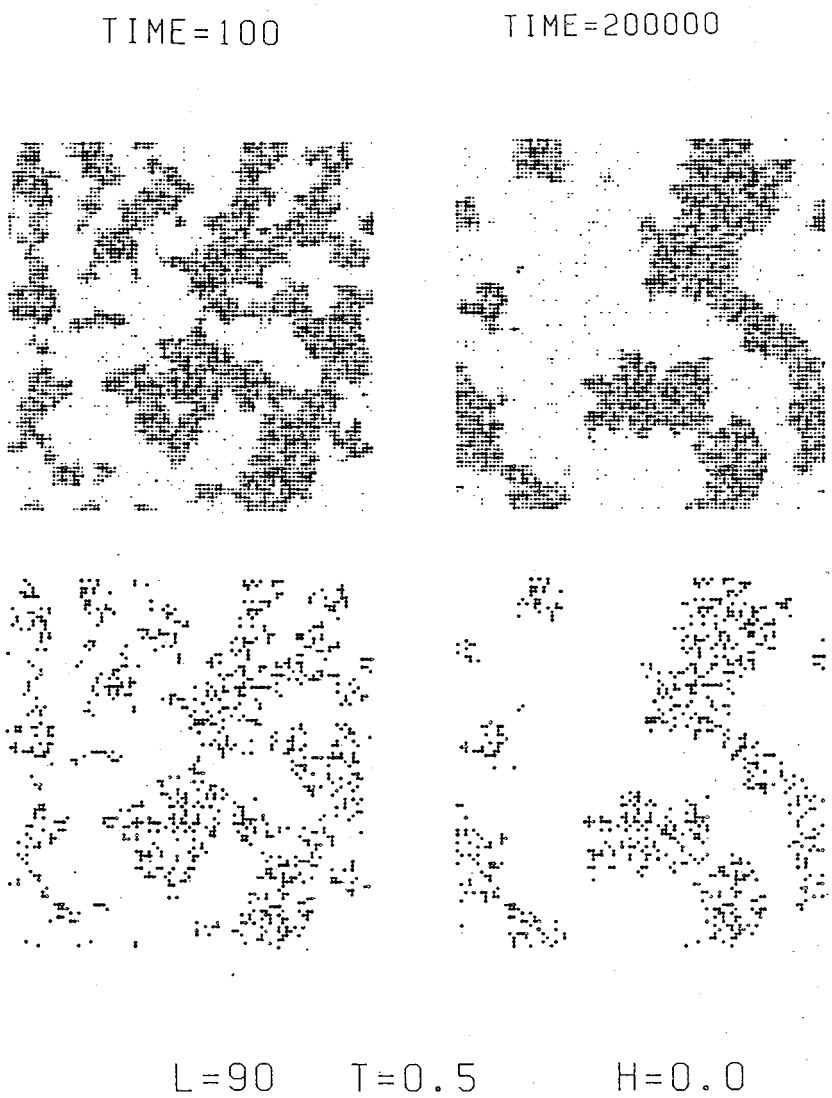

Fig. 12. Comparison between patterns before and after annealing. The map at 100 MCS is used as a reference of the original pattern since the map at 0 MCS has many unstable spins to annealing at the beginning.

To display the microscopic stability of the pattern, persistency of the individual spin direction is examined in the following scheme; as was in the first paragragh of this section, flipping possibility of the spins is estimated for three classes of spin magnitude and are tabulated in Table II for the lattice (90×90). The term 'initial' means the virgin state obtained after the 0-TQ and not processed further. The values tabulated denote ratios of unflipped spins after processed on the basis of the beginning (before quenching) configuration. (We counted number of spins only at the end and did not care whether the flipped or not during the course of annealing.) The bigger spins are found significantly hard to flip once their directions are stabilized by forming domains. The ratios become steady above 1×10^5 MCS below the ordering tempera-

Table II. Fraction of unflipped spins after annealing. Annealing the configuration obtained by the 0-temperature quenching is performed for 2×10^5 MCS in the lattice 90×90 at the temperatures indicated in the top line of the Table. Below the ordering temperature the bigger spins apt to keep their directions for a long time which may assure the original pattern.

Spin Magnitude	initial	$0.1J$	$0.3J$	$0.5J$	$1.1J$
Big	0.66	0.63	0.59	0.57	0.50
Mid	0.48	0.51	0.48	0.47	0.51
Sml	0.51	0.57	0.52	0.49	0.52

ture. Some trials show that the equilibrium state is not achieved even after 8×10^5 MCS. The value 0.50 means flipping possibility is about fifty-fifty. We have not estimated individual spin-spin correlations for these classes of spins to figure out the stability of the patterns since they are not directly associated with physical quantities.

§ 5. Discussion

We have shown that the random spin system introduced here is rich in almost degenerated metastable states and examined stability of the states from the microscopic point of view. Randomness in spin magnitude is one of the most essential factors for the system to have heavily degenerated metastable states, associating with results in other random systems.[4] Hardness in flipping of the bigger spins is found to contribute to toughness of the states against disturbances. Though a variety of spin magnitudes prevents the existence of truely free spins that favors degeneracy of the states, it does help to make significant barriers among the metastable states. Some barriers persist for a fairly long time, compared with that of the standard Ising system, below the ordering temperature.

Determination of T_c

Temperature dependence of spontaneous magnetization is plotted in Fig. 13, with that of the mean-field theory and the exact one of the Ising model. The magnetization here is calculated as square-root of the magnetic correlation $\langle MM\rangle$. To fit the curves with each other, determination of the ordering temperature T_c is crucial. First rough estimation is done by the curve of the spin-glass order parameter in Fig. 6. The ordering temperature will lie between $1.0J$ and $1.05J$. Other thermal quantities are also simulated with cooling and annealing by the step of $0.025J$ from $T=1.4J$ toward lower temperatures. At each step the system is annealed for 5×10^5 MCS and first 10^5 MCS are discarded before thermal averaging. Near the guessed T_c ($=1.034J$), we found however that the annealing time was not necessarily enough to get the true equilibrium at some temperature steps. Therefore we found, from the present insufficient data, only a tendency that the total magnetization has a constant sign below $T=1.025J$ for more than 5×10^5 MCS: Above $T=1.050J$ it changes sign several times in the same period. We therefore guess the ordering temperature will be between $1.025J$ and $1.050J$.

The ordering temperature is also determined by assuming the critical indices

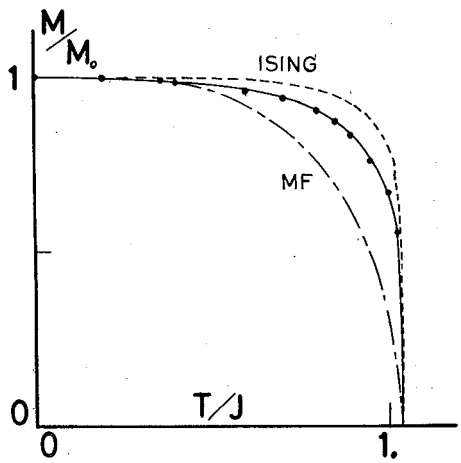

Fig. 13. Spontaneous magnetization. Solid line indicates the present result; dashed line shows the exact result of the Ising model and dash-dotted one is from the molecular field theory with $s=1/2$.

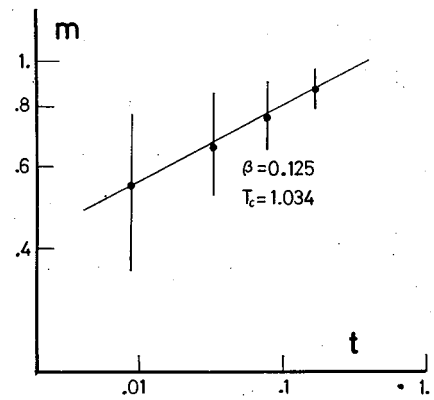

Fig. 14. Critical index β versus scaled temperature $t(\equiv|T-T_c|/T_c)$. Near T_c there needs more data to get reliable determination.

should be the same as those of the Ising model though there are many discussions about modifications on the indices of the random systems.[11)~13)] Detailed discussion on the index will remain as a future problem. As is shown in Fig. 14, the index $\beta=1.25$(Ising) enjoys best fit to the data scaled with $T_c=1.034$: $\beta=1.30$ for $T_c=1.033$ and $\beta=1.21$ for $T_c=1.035$. Concerning indices above T_c, we cannot say anymore at present. The data show more than 10^6 MCS are required before averaging.

Acknowledgements

The author would like to thank Professor O. Nagai for valuable discussions and comments, who kindly sent the author the results presented in the Appendix. He also thanks Professor S. Miyashita for kind discussions and advice on numerical analysis, in particular on vectorizing the Fortran programs.

Appendix

First we rewrite the Hamiltonian (1) as follows:

$$H=-\sum_{<ij>}J_{ij}S_iS_j\sigma_i\sigma_j\,, \tag{A·1}$$

where S_j takes only positive values between 0 and S randomly and σ_j carries only its sign. Then the partition function is calculated as:

$$Z=\sum_{\sigma_i=\pm1}\cdots\sum_{\sigma_N=\pm1}e^{-H/k_BT} \tag{A·2}$$

$$=\sum_{\sigma_i=\pm1}\cdots\sum_{\sigma_N=\pm1}e^{J\Sigma_jS_jS_{j+1}\sigma_j\sigma_{j+1}/k_BT}$$

$$=\sum_{\sigma_1=\pm1}\cdots\sum_{\sigma_N=\pm1}\prod_j\{\cosh K_j+\sigma_j\sigma_{j+1}\sinh K_j\}$$

$$=2^N\{\prod_j\cosh K_j+\prod_j\sinh K_j\} \tag{A·3}$$

since

$$e^{S_jS_{j+1}\sigma_j\sigma_{j+1}}=\begin{cases}e^{K_j} & \text{for } \sigma_j\sigma_{j+1}=+1\,,\\ e^{-K_j} & \text{for } \sigma_j\sigma_{j+1}=-1\,,\end{cases} \tag{A·4}$$

where

$$K_j=\frac{J}{k_BT}S_jS_{j+1}\,. \tag{A·5}$$

For large N, we will get

$$Z=2^N\prod_j\cosh K_j\,. \tag{A·6}$$

Therefore the free energy is given by

$$F=-k_BT\langle\log Z\rangle_c\,, \tag{A·7}$$

$$=-Nk_BT\log 2-k_BT\langle\sum_j\log\cosh K_j\rangle_c\,, \tag{A·8}$$

where $\langle\cdots\rangle_c$ indicates the configuration average. Using the distribution function of spins $h(S)$, the average is defined by

$$\langle f(S_1,\,S_2,\cdots,\,S_N)\rangle_c=\int_0^1dS_1\int_0^1dS_2\cdots\int_0^1dS_Nh(S)f(S_1,\,S_2,\cdots,\,S_N)\,. \tag{A·9}$$

Then we will get analytic expessions of internal energy and specific heat:

$$E=-J\sum_j\langle S_jS_{j+1}\tanh K_j\rangle_c \tag{A·10}$$

$$\to-NJS^2\int_0^1dx_1\int_0^1dx_2x_1x_2h(x_1,x_2)\times\tanh\frac{Jx_1x_2S^2}{k_BT}\,, \tag{A·11}$$

$$C=\frac{J}{k_BT^2}\sum_j\left\langle\frac{S_j^2S_{j+1}^2}{\cosh^2K_j}\right\rangle_c \tag{A·12}$$

$$\to\frac{NJS^2}{k_BT^2}\int_0^1dx_1\int_0^1dx_2\times h(x_1,x_2)\frac{x_1^2x_2^2}{\cosh^2\frac{Jx_1x_2}{k_BT}}\,. \tag{A·13}$$

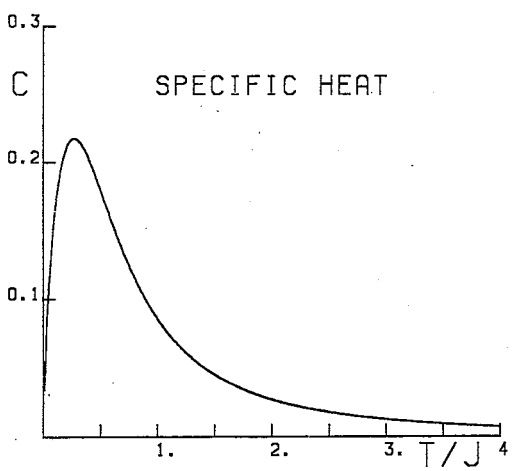

Fig. A1. Specific heat in the fuzzy chain model.

These expressions are identical with those of the standard Ising model when we set $h(x)=x_j=1$: The Shottocky-type

anomaly is seen in the specific heat, as is shown in Fig. A1. A similar behavior is expected for the other distribution function $h(x)$ as far as there are no magnetic defects.

References

1) T. Kawasaki, Prog. Theor. Phys. **80** (1988), 203.
2) T. Kawasaki, J. de Phys. **C8** (1988), 1015.
3) T. Kawasaki, *Cooperative Dynamics in Complex Physical Systems,* ed. H. Takayama (Springer-Varlag, Berlin, 1989), p. 223.
4) A. E. Jacobs and C. M. Coram, Phys. Rev. **B36** (1987), 3844.
5) S. Masui, B. W. Southern and A. E. Jacobs, Phys. Rev. **B39** (1989), 6925.
6) S. Masui, T. Li, B. W. Southern and A. E. Jacob, Phys. Rev. **B40** (1989), 7096.
7) M. Cieplak and T. R. Gawron, J. of Phys. **A20** (1987), 5657.
8) D. C. Mattis, Phys. Lett. **56A** (1976), 421.
9) F. Tanaka and S. F. Edwards, J. of Phys. **F10** (1980),2769.
10) K. Nemoto, J. of Phys. **A21** (1988), L287.
11) Vik. S. Dotsenko and Vl.S. Dotsenko, J. of Phys. **C15** (1982), L557; Adv. Phys. **32** (1983), 129.
12) B. N. Shalaev, Phys. Lett. **58** (1987), 2466.
A. W. W. Ludwig, Phys. Rev. Lett. **61** (1988), 2388.
R. Shankar, Phys. Rev. Lett. **61** (1988), 2390.
13) J. S. Wang, W. Selke, Vl. S. Dotsenko and V. B. Andreichenko, Europhys. Lett. **11** (1990), 425.